



Creation of a composite solar ultraviolet irradiance data set

Matthew T. DeLand¹ and Richard P. Cebula¹

Received 16 May 2008; revised 29 July 2008; accepted 14 August 2008; published 5 November 2008.

[1] Characterization of long-term solar ultraviolet (UV) irradiance variations is important for understanding the radiative forcing of Earth's atmosphere. Extending such a characterization to multidecadal timescales requires the merging of multiple satellite data sets. Currently available irradiance data sets show both absolute offsets and time-dependent differences that vary between spectral ranges. We have created a composite spectral UV irradiance data set with daily spectra covering the wavelength range 120–400 nm for the time period November 1978 to August 2005. A reference irradiance spectrum is used for normalization to remove absolute biases between instruments. We selected the best irradiance data set for each spectral and temporal interval based on intercomparisons between overlapping data sets and comparisons with proxy model predictions. The long-term behavior of the merged composite irradiance data set is consistent with expectations based on other solar activity indicators. There is no difference between the minimum values for solar cycles 21 and 22 within the uncertainty of the data, and the maximum irradiance values for cycle 23 are slightly lower than those observed for cycles 21 and 22. We also compare our composite data set with published synthetic irradiance data. These two data sets generally agree within $\pm 2\%$ over most spectral and temporal ranges. We hope to extend this data set in the future using measurements from the SORCE satellite.

Citation: DeLand, M. T., and R. P. Cebula (2008), Creation of a composite solar ultraviolet irradiance data set, *J. Geophys. Res.*, *113*, A11103, doi:10.1029/2008JA013401.

1. Introduction

[2] Solar ultraviolet (UV) irradiance is the primary energy source for the Earth's middle atmosphere, with most of the radiation in the wavelength range 190–300 nm deposited between 30–50 km [Meier, 1991]. Figure 1 shows that since 1978, a number of different satellite instruments have made continuous solar observations in the UV wavelength region. The Nimbus-7 Solar Backscatter Ultraviolet (SBUV) spectrometer measured solar activity from solar cycle 21 maximum to the minimum between cycles 21 and 22 [Schlesinger and Cebula, 1992; DeLand and Cebula, 2001]. The Solar Mesosphere Explorer (SME) also measured from cycle 21 maximum to the cycle 21–22 minimum [Rottman, 1988]. The NOAA-9 SBUV/2 instrument observed the full range of solar cycle 22 [DeLand *et al.*, 2004a], while the NOAA-11 SBUV/2 instrument measured the maximum and declining phase of solar cycle 22 [Cebula *et al.*, 1998; DeLand and Cebula, 1998]. The Upper Atmospheric Research Satellite (UARS) Solar Ultraviolet Spectral Irradiance Monitor (SUSIM) [Floyd *et al.*, 2002] and UARS Solar Stellar Intercomparison Experiment (SOLSTICE) [Rottman *et al.*, 2001] instruments observed the Sun from the maximum of solar cycle 22 through the declining phase of solar cycle 23.

[3] Examination of Figure 1 shows that only a few solar spectral irradiance instruments have made observations over even one complete solar cycle. This limitation complicates efforts to study solar irradiance variations over multidecade timescales, because the continuity of the data record must be established. The ability to understand terrestrial climate variations will be improved if a unified, self-consistent spectral irradiance data set is available to climate researchers [e.g., Crooks and Gray, 2005; Bengtsson, 2006]. Our goal is to create a composite solar spectral irradiance data set for the wavelength range 120–400 nm, covering the time period from November 1978 through August 2005.

[4] Some instruments shown in Figure 1 do not have complete corrections for long-term throughput changes, and so their data will not be considered in this report. This subset includes the Global Ozone Monitoring Instrument (GOME) [Weber *et al.*, 1998]; the NOAA-16, NOAA-17, and NOAA-18 SBUV/2 instruments; and the Scanning Imaging Absorption Spectrometer for Atmospheric Cartography (SCIAMACHY) [Skupin *et al.*, 2005]. Fully calibrated UV irradiance data are now being distributed from the Solar EUV Experiment (SEE) on the Thermosphere Ionosphere Mesosphere Energetics and Dynamics (TIMED) satellite [Woods *et al.*, 2005], and from the Spectral Irradiance Monitor (SIM) and SOLSTICE II instruments on the Solar Radiation and Climate Experiment (SORCE) satellite [Rottman, 2005]. We hope to make use of these data in the future.

¹Science Systems and Applications, Inc., Lanham, Maryland, USA.

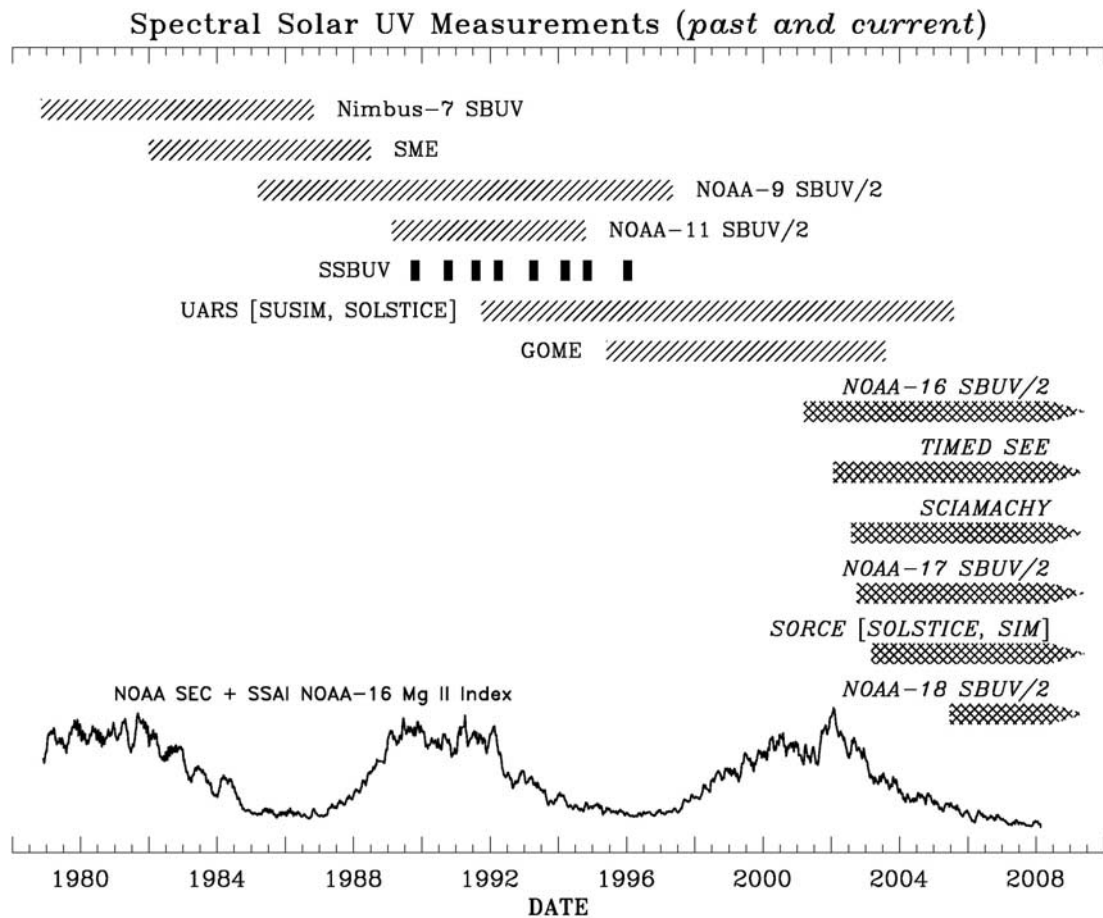


Figure 1. Timeline of satellite solar UV irradiance measurements since 1978. Active instruments are shown with arrowheads. The Mg II index data from *Viereck and Puga* [1999], extended through April 2008 with recent measurements from the NOAA-16 SBUV/2 instrument, are shown for reference.

[5] Previous efforts to construct composite solar activity data sets have included total solar irradiance (TSI) [Fröhlich, 2006; Willson and Mordvinov, 2003; Dewitte et al., 2004], Lyman alpha flux [Woods et al., 2000], and the Mg II proxy index [DeLand and Cebula, 1993; Viereck and Puga, 1999; Viereck et al., 2004]. The creation of a composite spectral irradiance data set poses additional challenges beyond those faced in creating a composite TSI or Mg II index product because of the spectral range of the data and the increased importance of instrument degradation corrections. Figure 2 shows a time series of published irradiance data averaged over 200–205 nm from the instruments listed in Table 1. Approximately 11-year solar cycle variations are seen in all of the data sets, as well as rotational modulations (~27-day period) that cannot be resolved in this plot. However, there are some other points that should be noted.

[6] 1. Absolute offsets are observed between any two instruments, with different values depending on the pair of instruments chosen. In addition, wavelength-dependent variations in the offset values appear when a different set of wavelengths (e.g., 235–240 nm) is used.

[7] 2. Time-dependent comparisons between two overlapping data sets can show relative changes that are difficult to ascribe to either instrument. The nature of this drift

frequently changes magnitude and temporal location for different parts of the overall spectral region.

[8] 3. Each instrument has a different native resolution, which can lead to significant differences in observed irradiances near rapidly varying spectral features.

[9] We discuss our approach to treating each of these issues in the following sections. Section 2 describes the nature of the individual instrument data sets and our efforts to standardize them. Section 3 discusses the evaluation of individual data sets using time series of irradiance data. Section 4 describes the specific steps involved in creation of the composite irradiance data set, including data selection, data gap filling, and creation of the source flag. Section 5 presents some evaluation and validation of this data set, using both internal comparisons and external data sets. Section 6 presents conclusions, identifies remaining issues, and discusses future plans.

2. Data Sets

2.1. Input Data Sets

[10] In order to simplify comparison and merger of data sets for the composite spectral irradiance product, we use only the publicly released data sets for each instrument listed in Table 1. Each data set has been fully characterized

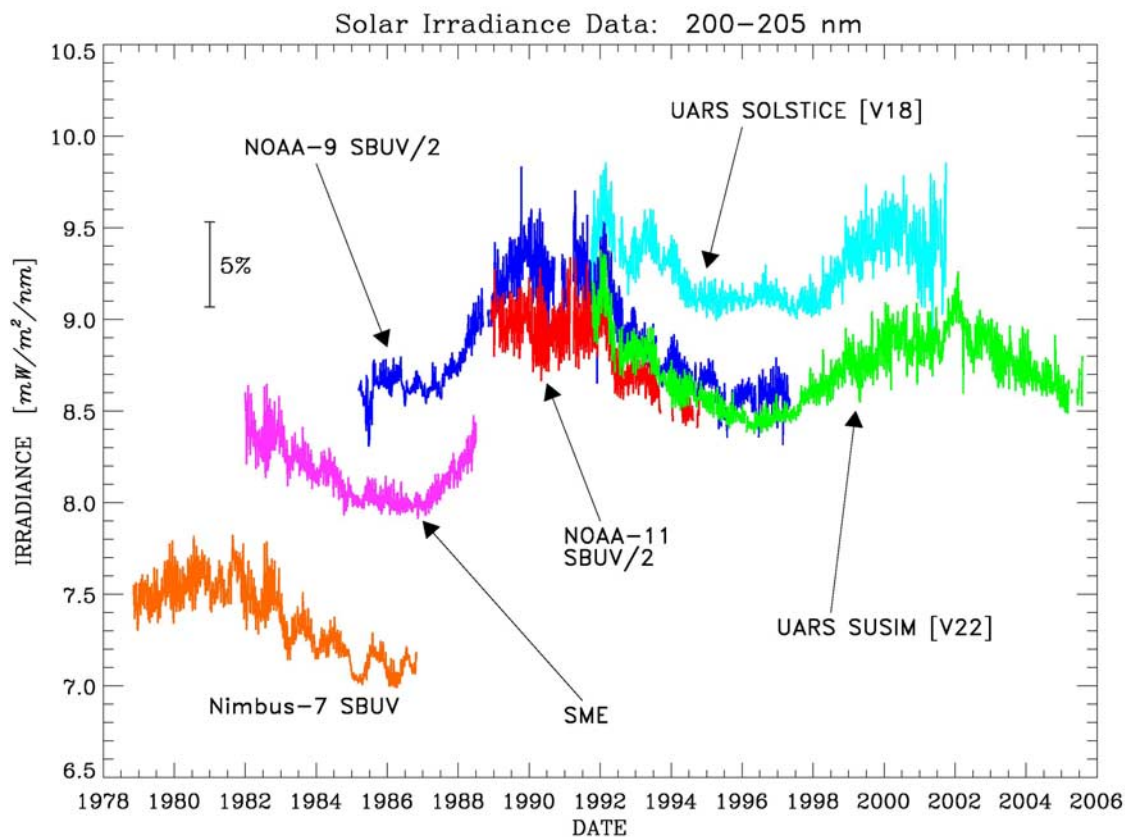


Figure 2. Time series of published solar irradiance data sets averaged over 200–205 nm. No absolute adjustments have been applied.

and corrected for long-term instrument response changes by the respective authors. The format of each data set is daily average irradiance spectra (corrected to 1 AU), provided in 1 nm bins on 0.5 nm centers over the wavelength range listed (e.g., 170.5, 171.5, ...399.5 nm for Nimbus-7 SBUV). The wavelength range of the final composite irradiance product is limited to 120–400 nm, even though some instruments have slightly more coverage in their native data sets. Nimbus-7 SBUV, NOAA-9 SBUV/2, and NOAA-11 SBUV/2 data have been converted to this format. All data sets incorporate the best efforts by instrument teams to correct for long-term throughput changes. Table 1 lists basic reference information about each instrument.

2.2. Normalization

[11] We would like to have all individual irradiance data sets on the same absolute scale to facilitate later steps in the composite process (such as joining, averaging, etc.). Each

instrument uses its own process for establishing the absolute calibration, although some intercomparisons have been presented previously [Cebula *et al.*, 1991; Woods *et al.*, 1996; Cebula *et al.*, 1996; DeLand *et al.*, 2004b]. Rather than tie everything to a single instrument, we have chosen to use the reference spectrum by Thuillier *et al.* [2004] for the ATLAS-1 Shuttle flight on 29 March 1992 as a baseline for this step. The relevant portion of this data set for our work is shown in Figure 3. The ATLAS-1 reference spectrum was recorded at a relatively high solar activity level ($F_{10.7} = 192$), and is concurrent with measurements from four of the six instruments listed in Table 1 (NOAA-9, NOAA-11, SUSIM, SOLSTICE). This means that a comparison between the daily spectrum from any of these instruments on 29 March 1992 and the reference spectrum does not require any adjustment for differences in solar activity, which is important at wavelengths less than 300 nm. The original

Table 1. Instrument Summary for Data Sets Used in This Work

Instrument	Wavelength Range (nm)	Instrument Resolution (nm)	Time Period for Spectral Solar Data	References
Nimbus-7 SBUV	170–400	1.1	7 November 1978 to 28 October 1986	Schlesinger and Cebula [1992]; DeLand and Cebula [2001]
SME	115–302	0.8	1 January 1982 to 30 June 1988	Rottman [1988]
NOAA-9 SBUV/2	170–400	1.1	14 March 1985 to 5 May 1997	DeLand <i>et al.</i> [2004a]
NOAA-11 SBUV/2	170–400	1.1	2 December 1988 to 15 October 1994	Cebula <i>et al.</i> [1998]; DeLand and Cebula [1998]
UARS SUSIM [V22]	115–410	1.1 [daily spectra]	12 October 1991 to 31 July 2005	Floyd <i>et al.</i> [2002]
UARS SOLSTICE [V18, 2005]	119–419	0.2	3 October 1991 to 30 September 2001	Rottman <i>et al.</i> [2001]

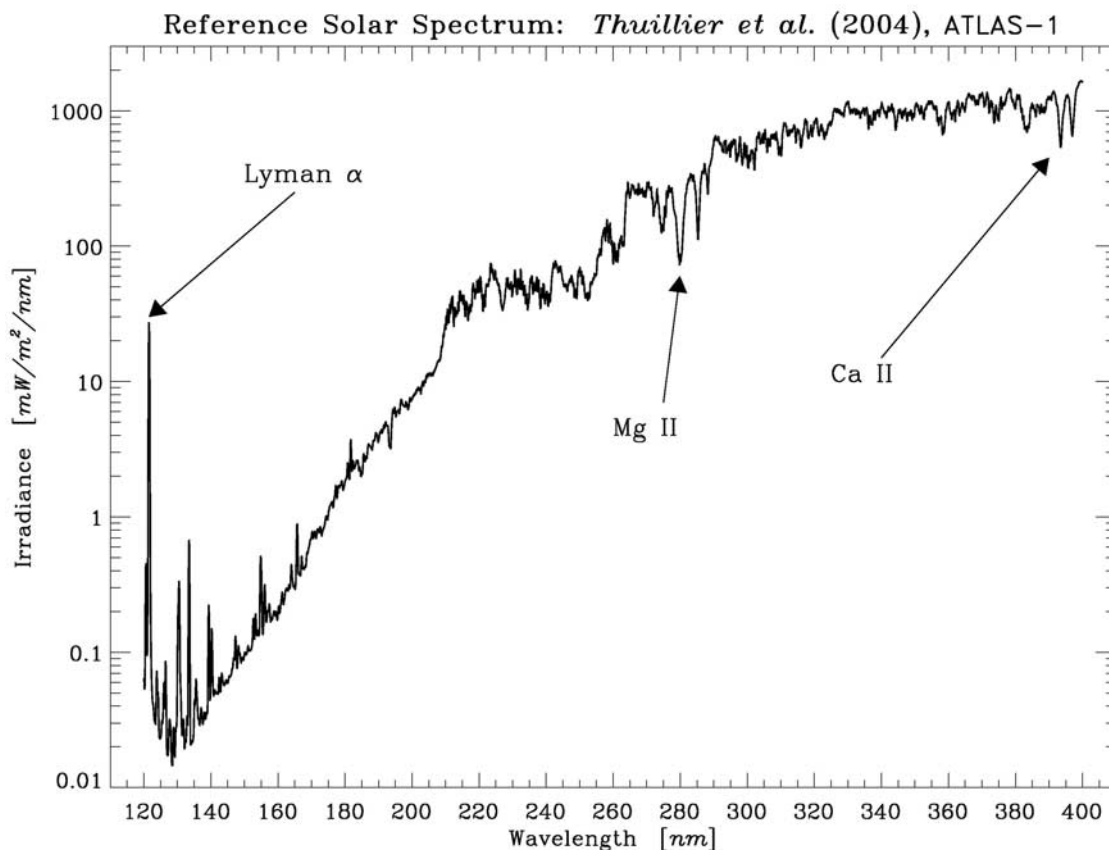


Figure 3. The reference solar irradiance spectrum of *Thuillier et al.* [2004] at full resolution ($\Delta\lambda = 0.25$ nm) over the wavelength range 120–400 nm as constructed for the ATLAS-1 Shuttle flight (29 March 1992).

spectrum by *Thuillier et al.* [2004] is provided at very high sampling ($\Delta\lambda = 0.25$ nm), so we also rebinned these data to 1 nm sampling for use here.

[12] The Nimbus-7 and SME data sets do not overlap with the ATLAS-1 reference spectrum, so a modified procedure is required to select a comparison date. We have identified dates in each data set with comparable solar activity, as determined by the NOAA SEC Mg II index [*Viereck and Puga, 1999*]. We required agreement with the 29 March 1992 Mg II value to within $\pm 0.3\%$ in the daily Mg II index and $\pm 0.1\%$ in the 81-day smoothed Mg II index to ensure that short-term fluctuations did not cause an inappropriate date to be selected. These criteria gave at least 10 candidates for each instrument. An example of the data selection process for non-overlapping instruments is shown in Figure 4. We selected the irradiance spectrum on 1982 day 279 for Nimbus-7 and SME normalization calculations. This date also has relatively high solar activity ($F_{10.7} = 152$) and occurs on the descending phase of the solar cycle, consistent with the ATLAS-1 reference spectrum.

[13] Previous comparisons of solar UV irradiance spectra from different satellite instruments have found that irradiance ratios often exhibit significant high frequency noise in the spectral direction. Figure 5 shows an example of this situation for the ratio between the UARS SOLSTICE spectrum and the spectrum by *Thuillier et al.* [2004]. This is typically attributed to slight inaccuracies in the original

wavelength scale of either or both instruments, compounded by the Fraunhofer absorption line structure that pervades the FUV and MUV spectrum. In addition, the UARS SOLSTICE instrument has a higher resolution than the other instruments used to construct the spectrum by *Thuillier et al.* [2004], so that creating a 1 nm binned irradiance product requires averaging more observed spatial structure. However, the spectral dependence of the absolute calibration difference is more likely to have broad features [e.g., *Woods et al., 1996; Cebula et al., 1996*]. We therefore chose to create a smoothed version of each instrument’s normalization ratio for operational use. After some testing, we selected a smoothing width of 5 nm to create the normalization ratios. Local differences between the unsmoothed and smoothed curves may or may not represent real irradiance differences, and will be discussed further in section 3.1. The spectrally dependent structure in these smoothed ratios is generally $\pm 5\%$ or less for NOAA-9, NOAA-11, SUSIM, and SOLSTICE, although SUSIM does have larger fluctuations at $\lambda < 140$ nm. The oldest two instruments have larger calibration differences from the reference spectrum: up to 10–20% for Nimbus-7 at $\lambda < 300$ nm, up to -20% for SME at 140 nm and larger at shorter wavelengths. The normalization ratio for these instruments is not sensitive to the choice of reference date. All of the 14 irradiance ratios available for Nimbus-7 SBUV comparisons with ATLAS-1 agree to within approximately 1% over the full wavelength

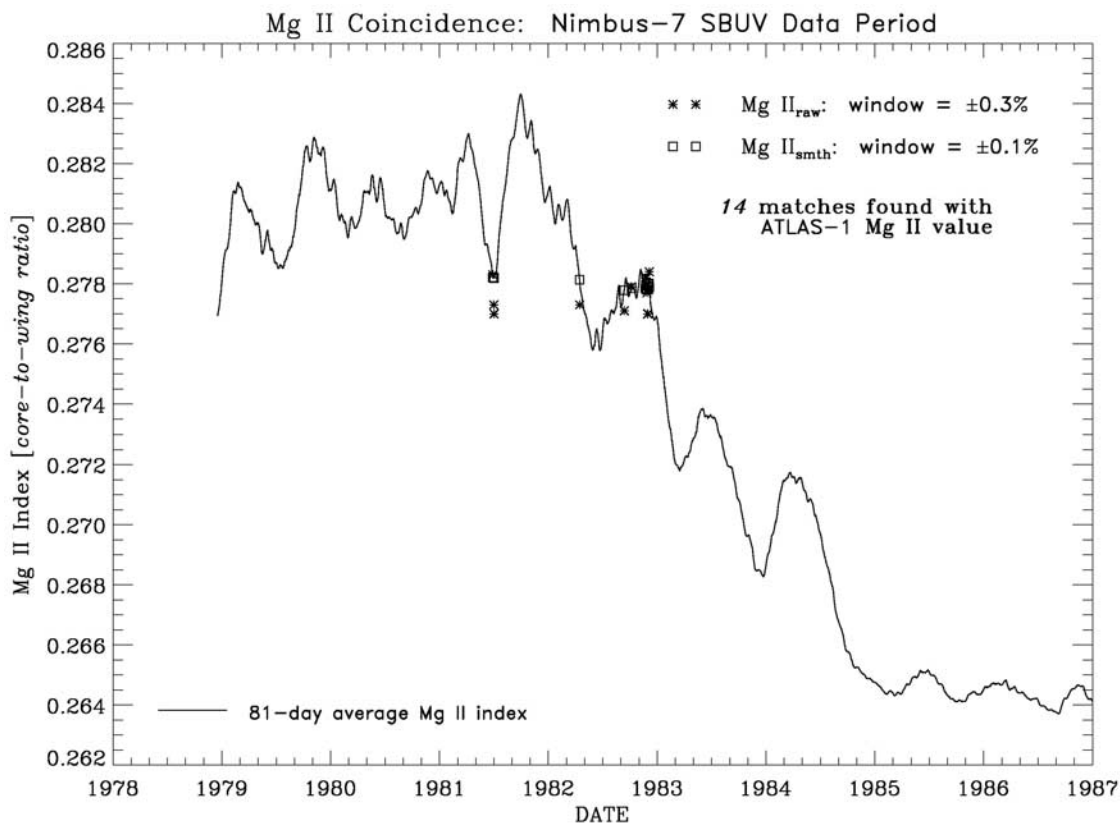


Figure 4. Example of the selection of a normalization date for an instrument that has no temporal overlap with the reference spectrum of *Thuillier et al.* [2004]. The plot shows the composite Mg II index smoothed with an 81-day average for clarity. In this example, comparison of the Nimbus-7 SBUV measurement period (November 1978 to October 1986) with the ATLAS-1 reference date (29 March 1992) found 14 dates whose unsmoothed Mg II values agreed with the reference data to within $\pm 0.3\%$ (*asterisk*), and whose 81-day smoothed Mg II values also agreed with the reference date to within $\pm 0.1\%$ (*square*).

range, and typical agreement is better than 0.5%. For comparison, the scatter between total solar irradiance (TSI) values for these same dates is $\pm 0.07\%$.

3. Data Set Evaluation

3.1. Time Series: Inter-Instrument Differences

[14] Time periods where more than one instrument has irradiance data requires a determination of how to create the final product for public distribution. Options include selecting a single instrument, averaging all available data equally, and combining the data sets in some predetermined weighted manner. In order to evaluate these options, we have compared irradiance time series in small spectral bands during all overlap periods between any two instruments. Taking all overlap combinations of the six data sets, and using $\Delta\lambda = 5$ nm, we have 378 comparison plots to examine.

[15] Figure 6 is a typical plot comparing irradiance data at 240–244 nm during 1991–1997. Data from NOAA-9 SBUV/2 are shown in Figure 6a, and data from UARS SOLSTICE are shown in Figure 6b. To create these time series, each daily average spectrum is divided by the appropriate normalization curve from the previous section,

and then the irradiance time series is extracted. The text indicating “absolute shift” represents the change in absolute irradiance for this wavelength band as a result of the normalization procedure. The Y-axis scale for each image is normalized to the start of observations for each instrument, so the limited section of data shown may be slightly offset from 1.0. These images show the overall level of solar activity during the overlap period, and also indicate whether one instrument has more day-to-day noise.

[16] Figure 6c shows the percent difference between absolute irradiance values after each data set has been adjusted, with a 5-day running average applied for clarity. If the adjustment procedure used in section 2.2 was accurate, we would expect these values to lie near zero. An offset can indicate that the adjustment procedure was not completely accurate, or that one instrument drifted prior to the start of the overlap period. Some time-dependent features that appear in this image (e.g., drifts, step changes) can be attributed to one instrument based on inspection of the raw data, but this identification is not always possible.

3.2. Time Series: Solar Proxy Comparison

[17] Further information about instrument behavior comes from comparison of the irradiance time series to

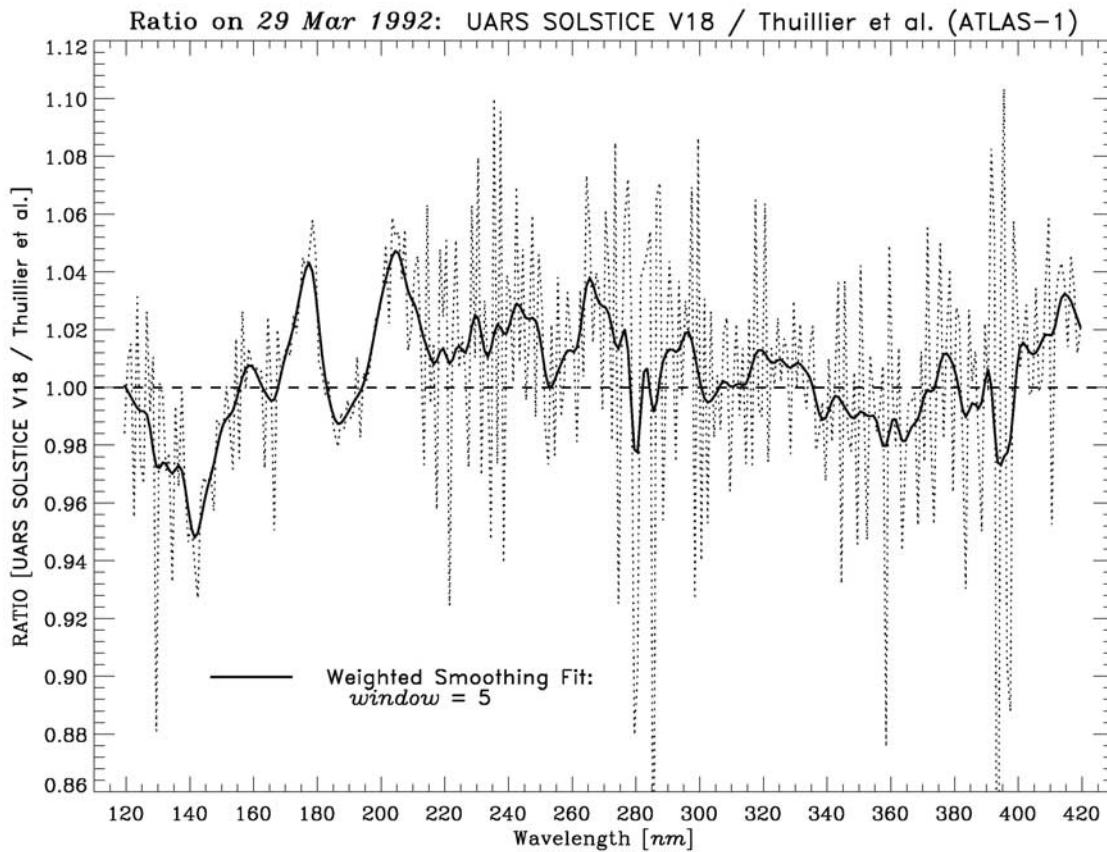


Figure 5. Ratio between UARS SOLSTICE data on 29 March 1992 and the spectrum of *Thuillier et al.* [2004]. Dotted line, unsmoothed irradiance ratio; thick line, weighted smoothing fit to data using 5-nm window. The smoothed irradiance ratio is used to adjust SOLSTICE data for creation of a merged irradiance product.

solar proxy predicted values. We use the 3-component model and contrast factors of *Woods et al.* [2000] for data between 120–170 nm, and the 2-component model and scale factors of *DeLand and Cebula* [1993] for data in the 170–300 nm region. The proxy scaling in the 2-component model (constant + daily Mg II values) was derived using solar rotational variations only, whereas the 3-component model includes an additional chromospheric network term based on 81-day averaged data. Comparison of these two models in the overlap region between 170–180 nm gives virtually identical results. Similar plots can be made for data between 300–400 nm, but the predicted solar activity in this wavelength range is so low that the difference calculation has no real value. This analysis is not intended to validate any individual data set based on comparisons to the proxy model prediction, but hopefully gives some guidance for attribution of any anomalies observed in the comparison plots of section 3.1.

[18] The sample plot in Figure 7 has the same format as the inter-instrument comparison plot, with normalized UARS SUSIM irradiance time series data at 150–154 nm shown in Figure 7a and proxy model predicted data shown in Figure 7b. The difference values in Figure 7c are now normalized to zero at the start of the record, since the proxy model values are calculated as relative changes. Omitting a

slight offset caused by the choice of normalization date, the irradiance data and proxy model values agree to within $\sim 2\%$. Previous studies that compare solar UV irradiance variations and proxy model values [e.g., *DeLand and Cebula*, 1998; *DeLand et al.*, 2004a, 2004b] indicate that this represents good agreement. The quasiperiodic variations in Figure 7c are small relative to the magnitude of the solar cycle variation at this wavelength, so it is difficult to determine whether they represent uncorrected instrument behavior errors or limitations in the proxy model characterization. Most wavelength bands between 150–300 nm show differences less than $\pm 3\%$ in these comparisons. Examples of problem areas with larger time-dependent drifts revealed by this analysis include Nimbus-7 SBUV data at $\lambda < 200$ nm in 1978–1979, and UARS SOLSTICE data at $\lambda = 240$ –270 nm after 1997. We tried to exclude such data whenever possible, while also avoiding the use of multiple small spectral and temporal intervals. The spectral region below approximately 150 nm is more difficult to evaluate with this approach because of the presence of both emission line structure in the irradiance spectrum and larger calibration uncertainties at these wavelengths. We find significant changes in behavior within a few nm spectrally in these data, and larger time-dependent fluctuations. This complicates

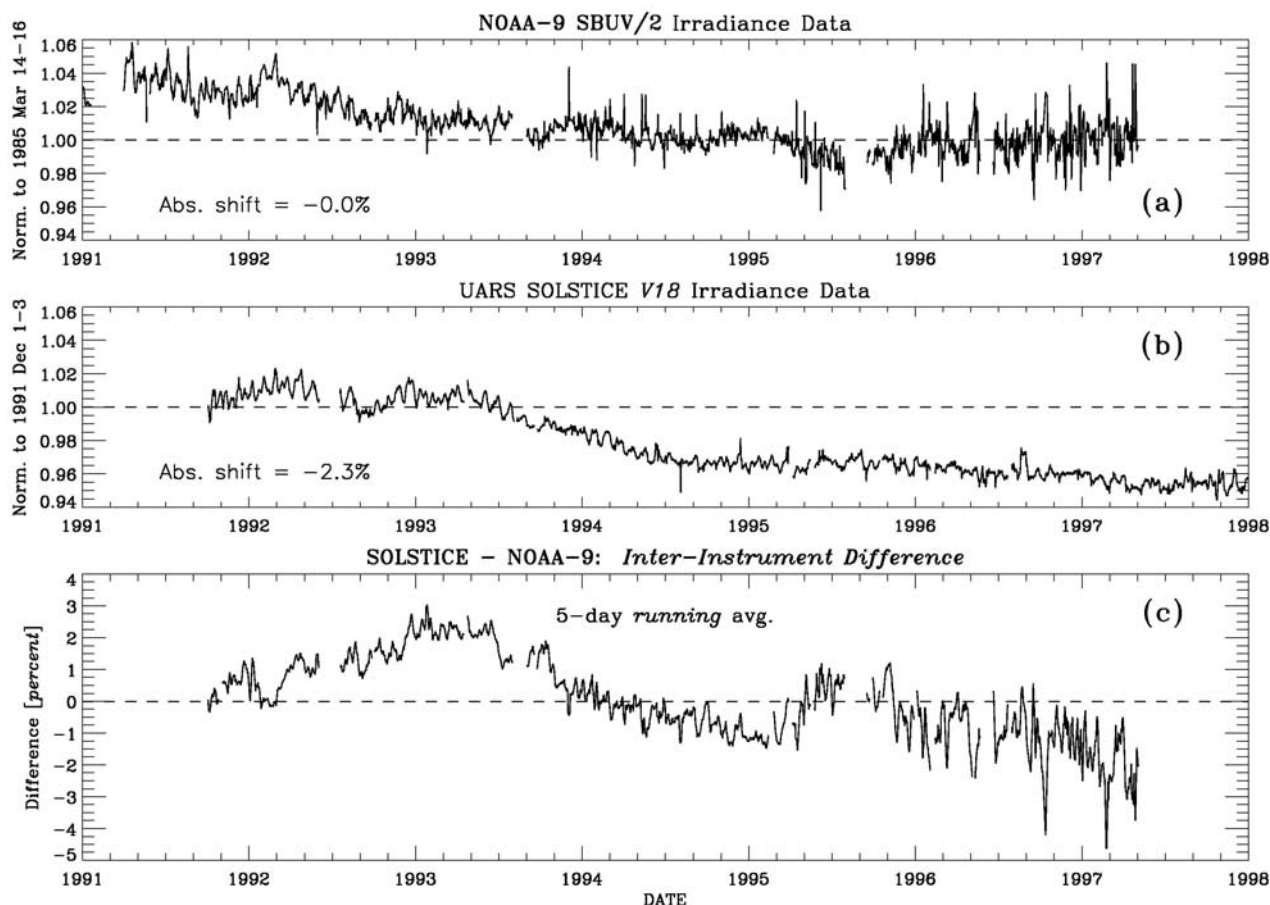


Figure 6. Solar irradiance data comparison at 240–244 nm for 1991–1998. (a) NOAA-9 SBUV/2 data, normalized to March 1985. The absolute shift value indicates the irradiance adjustment applied to this wavelength band as a result of the normalization process. (b) UARS SOLSTICE data, normalized to December 1991. The absolute shift value is defined as in Figure 6a. (c) Irradiance difference between SOLSTICE and NOAA-9 (in percent), smoothed with a 5-day running average. No additional normalization has been applied.

our effort to construct a coherent data set, as discussed in the next section.

4. Composite Spectral Irradiance Product

4.1. Selection of Data Sets for All Intervals

[19] The creation of the initial composite spectral irradiance data set has been performed using a single “best” instrument for each spectral and temporal interval. We chose to avoid averaging the data during periods of overlap because this requires a potentially complex assessment of relative data quality, as well as possible absolute irradiance steps when an instrument comes into or exits the average calculation. We have defined three spectral intervals for this portion of the process: 120–170 nm, 170–300 nm, and 300–400 nm. Within each spectral interval, different time periods have from zero to four data sets available. We tried to minimize the number of transitions, both spectral and temporal, whenever practical. Figure 8 shows the final set of assignments used. Major choices between instruments were made as follows.

[20] 120–170 nm:

[21] 1. SOLSTICE over SUSIM for December 1991 to September 2001. SUSIM data show frequent fluctuations of $\pm 10\%$ or more at $\lambda < 140$ nm.

[22] 2. SUSIM after September 2001. No other data available.

[23] 170–300 nm:

[24] 1. Nimbus-7 over NOAA-9 for 1985–1986. Better signal-to-noise in Nimbus-7 data.

[25] 2. NOAA-11 over NOAA-9 for 1989–1991. NOAA-11 has fewer issues with data gaps.

[26] 3. SUSIM over NOAA-11 (1992–1994), NOAA-9 (1992–1997), SOLSTICE (1992–2001). SUSIM data have good signal-to-noise performance, continuity for long period (through mid-2005).

[27] 300–400 nm:

[28] 1. NOAA-9 over Nimbus-7 for 1985–1986. NOAA-9 data have less drift.

[29] 2. NOAA-11 over NOAA-9 for 1989–1991. NOAA-11 has fewer issues with data gaps.

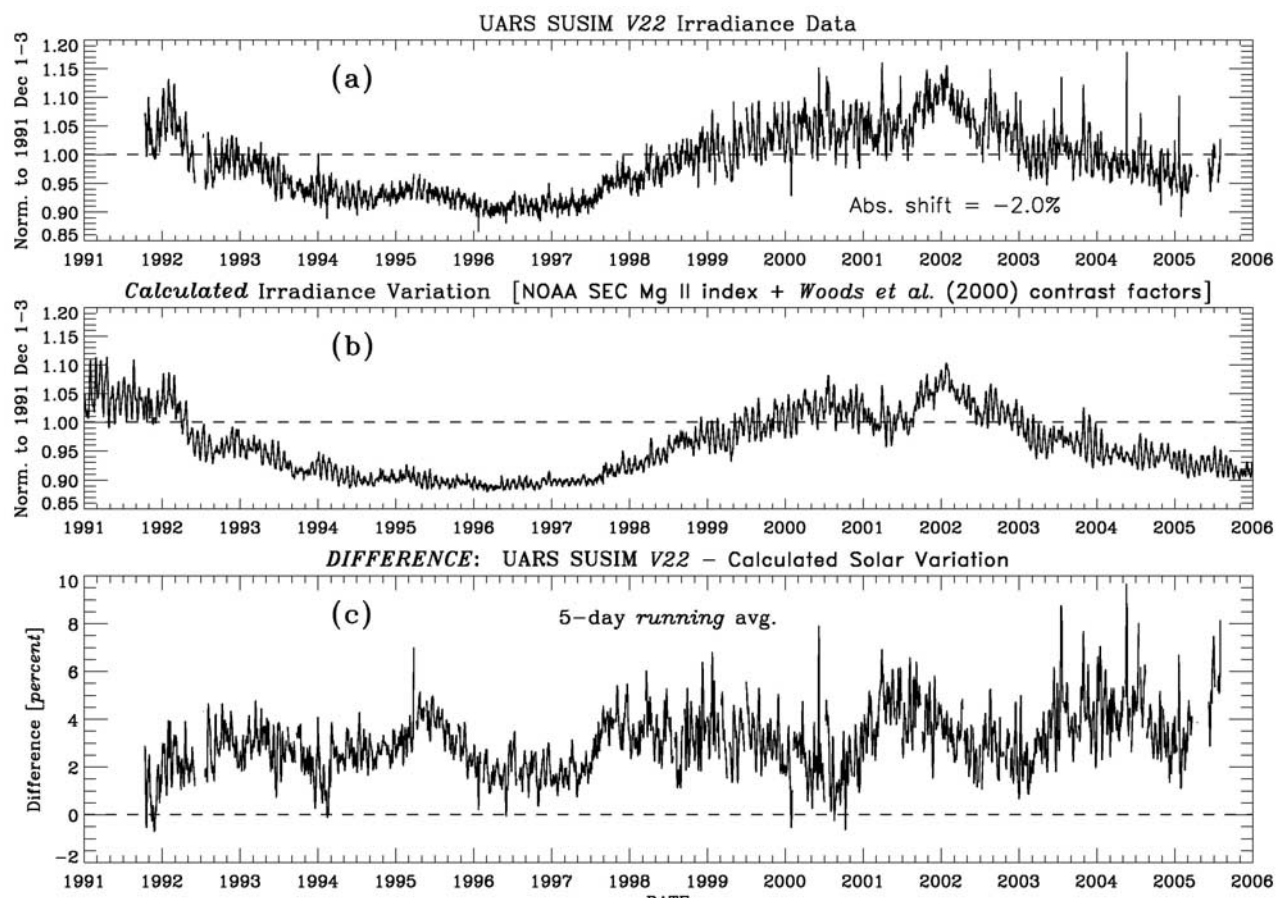


Figure 7. Solar irradiance data and proxy value comparison at 150–154 nm for 1991–2006. (a) UARS SUSIM data, normalized to December 1991. The absolute shift value indicates the irradiance adjustment applied to this wavelength band as a result of the normalization process. (b) Predicted irradiance variation using the contrast model of *Woods et al.* [2000]. (c) Relative irradiance difference between SUSIM data and calculated proxy values (in percent), smoothed with a 5-day running average.

[30] 3. SUSIM over NOAA-11 (1992–1994), NOAA-9 (1992–1997), SOLSTICE (1992–2001). SUSIM data have good signal-to-noise performance, continuity for long period (through mid-2005). SUSIM data are not forced to be flat.

[31] Tables A1–A3 in Appendix A give more detailed descriptions of the data sets available for each time period in each of the major spectral intervals, as well as the comparative information that was used in making the final selection.

4.2. Filling of Data Gaps

[32] The overall spectral irradiance data record for the wavelength range 120–400 nm and the time period November 1978 to June 2005 is far from complete. The most obvious problems are multiyear periods where no measurements were made at 120–170 nm (November 1978 to December 1981, July 1988 to November 1991). On a shorter timescale, there are numerous periods ranging in length from weeks to months (e.g., September to November 1988, March 1991, June 1992) where observations from the primary (or only) instrument are not available, and a spline interpolation (discussed below) is not appropriate. Table 2 lists all gaps greater than 10 days that are filled in the final irradiance product. Finally, there are many gaps ranging

from one day to a few days, particularly for Nimbus-7 SBUV in 1979–1983 (instrument power shutdown) and UARS SUSIM in 2002–2005. A variety of methods have been used to treat these data gaps.

[33] Cubic spline interpolation in time provides the simplest way to fill short gaps in the data set with values that are consistent with the immediate history of the neighboring measurements, assuming that the data are not too noisy. However, extending the size of gaps treated with this method also runs the risk of creating synthetic data that ignore short-term solar variations, such as rotational modulation with an approximate 27-day period. Therefore the initial composite irradiance data set only uses spline interpolation to fill all data gaps up to 10 days in length. *Viereck et al.* [2004] used a similar procedure in creating their composite Mg II index data set. This approach is applied to the time series data for each 1 nm spectral bin individually.

[34] We realize that this approach may fail to capture some short-term solar variations, such as when a data gap coincides with a rotational maximum or minimum, or when 13-day periodicity is present. However, reducing the maximum interpolation interval greatly increases the number of “large” data gaps that should be filled with proxy data, as described in the next paragraph. Since that approach also

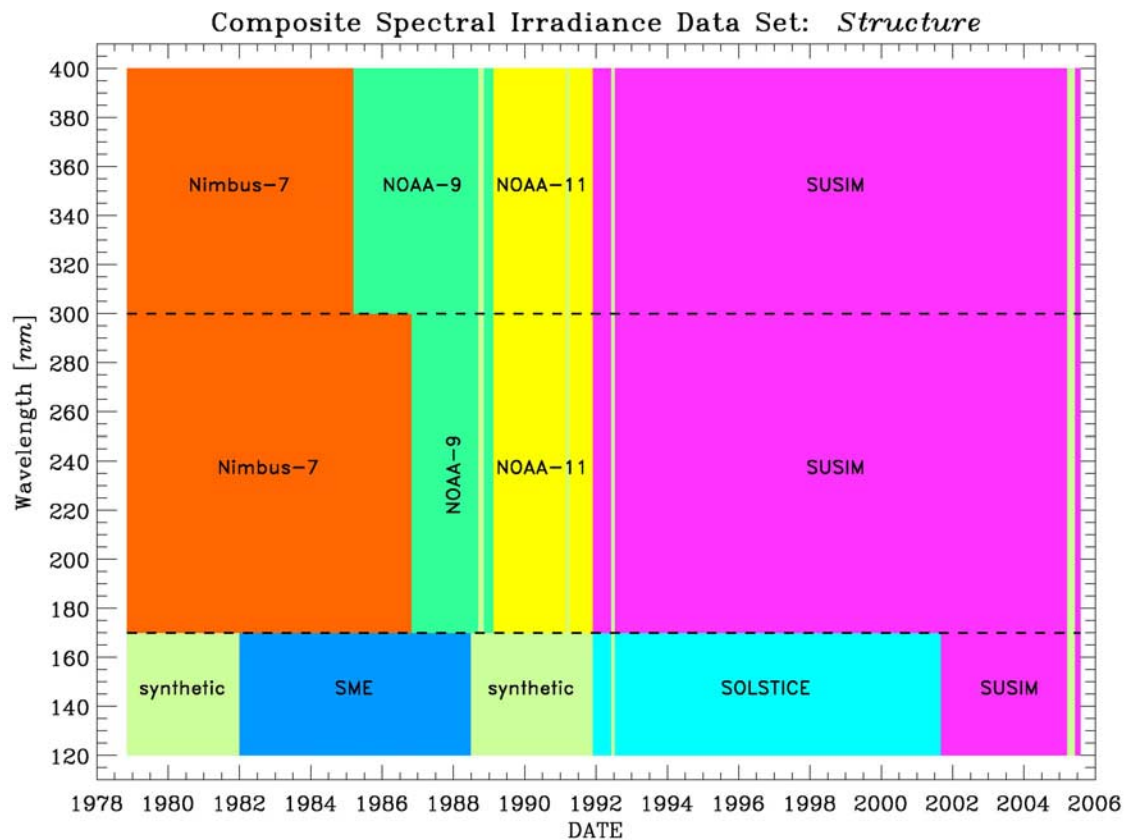


Figure 8. Instrument selections for each spectral and temporal interval in the composite spectral irradiance data set, corresponding to the discussion given in Tables A1–A3. Intervals of synthetic data are shown in light green and correspond to the time periods listed in Table 2.

has limitations on accuracy, we have chosen to implement a relatively simple method. Experiments with techniques such as autoregression were not successful at all wavelengths, perhaps because of the combined effects of solar variations (which can be large compared with any short-term trend) and instrument noise.

[35] Larger data gaps should ideally be filled with some representation of solar activity, so the most obvious choice is to use the solar proxy models discussed in section 3.2. However, some significant data gaps also exist in the composite Mg II index maintained by NOAA SEC. These gaps can be filled by regression with an alternate solar UV proxy, such as 10.7 cm radio flux [Tapping, 1987] or He II 1083 nm equivalent width [Harvey, 1984]. The 10.7 cm flux data set is very complete temporally, but can also experience large short-term fluctuations due to its origin on the solar corona (up to a factor of two in a few days) that are not truly representative of FUV and MUV irradiance variations. The

He II 1083 nm data have more frequent gaps and limited accuracy because of the digitization of the product, but the physical source of the variability in the solar chromosphere is more consistent with both Mg II index and FUV/MUV irradiance variations. DeLand and Cebula [1993] provide further discussion of the relationship between 10.7 cm flux, He II 1083 nm equivalent width, and Mg II index data. We used regression fits between He II 1083 nm and Mg II index data over the period 1985–1997 to generate synthetic Mg II data and fill gaps greater than 10 days in the Mg II data set, and filled smaller gaps using cubic spline interpolation. Two He II 1083 nm data values in March 1991 were modified to correct an obvious error. Tests conducted with this procedure on data intervals where Mg II index data are available indicate that the accuracy of the synthetic Mg II index data should be approximately 0.5%, which is sufficient to represent short-term rotational modulation behavior. This

Table 2. Data Gaps of 11 or More Days for Which Synthetic Data are Created

Start and End Dates	Spectral Range (nm)	Cause for Data Gap
1978/311–1981/365	120–170	No measurements available
1988/182–1991/334	120–170	No measurements available
1988/257–1988/335	170–400	NOAA-9 SBUV/2 shadowed by spacecraft solar array
1991/060–1991/090	170–400	NOAA-9, NOAA-11 SBUV/2 Level 1B tapes lost
1992/155–1992/193	120–400	UARS satellite solar array problem
2005/080–2005/158	120–400	UARS SUSIM powered off
2005/189–2005/201	120–400	UARS SUSIM powered off

Table 3. Definitions for Data Source Flag Values

Flag	Definition
10	Nimbus-7 SBUV data
20	SME data
30	NOAA-9 SBUV/2 data
40	NOAA-11 SBUV/2 data
50	UARS SUSIM data
60	UARS SOLSTICE data
90	Proxy (synthetic) data
0	Raw data
1	Interpolated data
2	Manipulated data
6	Mg II index (from regression) + contrast factors
7	Mg II index (observed) + contrast factors
8	Mg II index (from regression) + scale factors
9	Mg II index (observed) + scale factors

enhanced Mg II index data set was then used to calculate proxy irradiance values as needed.

4.3. Creation of Irradiance Data Set

[36] The data in the composite spectral irradiance product clearly have a complex heritage, whether considered in

either a spectral or temporal sense. It is important for any user to understand this heritage so that they use the irradiance product with confidence and understand its limitations. We have developed a data source flag that accompanies each irradiance sample to explain its origin. The flag is a 2-digit number, where the first digit indicates the primary source, and the second digit indicates additional modifications. Table 3 summarizes the meaning of each flag value. The term “manipulated data” (FLAG = 2) is reserved for empirical adjustments (e.g., prescribed linear trend correction) that in general have not yet been defined or implemented. The only such adjustment used at this time is applied to quasi-annual variations in Nimbus-7 SBUV data, as described in the study of *DeLand and Cebula* [2001]. Further revisions to the observed irradiance data may be addressed in future work.

[37] For the initial version of the composite spectral irradiance data set, all observed irradiance values were incorporated using only the absolute adjustments described in section 2.2. Since the solar proxy methods produce relative changes from a defined reference point, a starting irradiance value must be specified. In situations where a

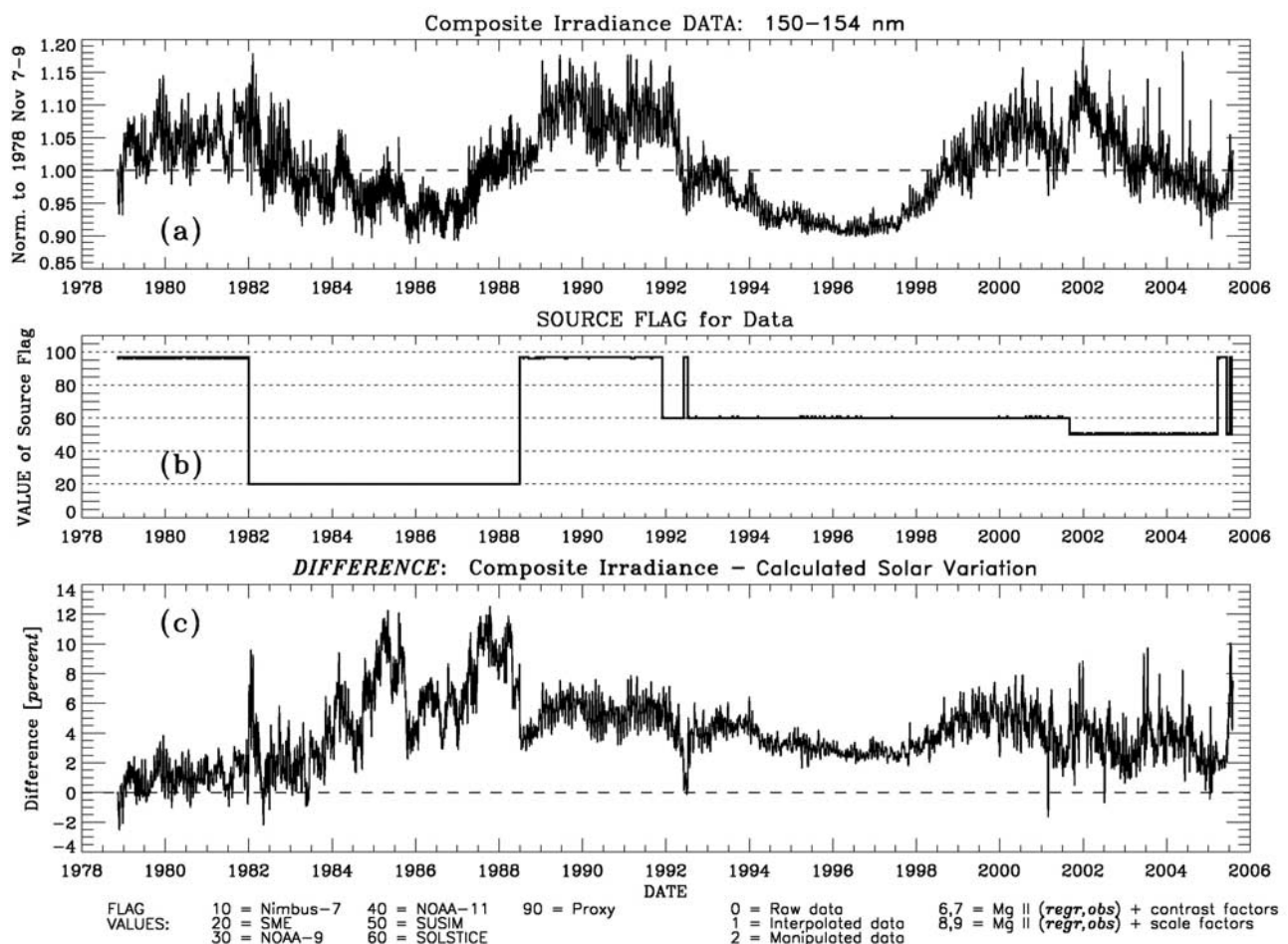


Figure 9. Composite spectral irradiance time series at 150–154 nm. (a) Irradiance data normalized to November 1978. (b) Data source flag for each daily sample. Table 3 describes the information contained in these flag values. (c) Relative irradiance difference between the composite irradiance data and calculated proxy values using the 3-component model (in percent), smoothed with a 5-day running average.

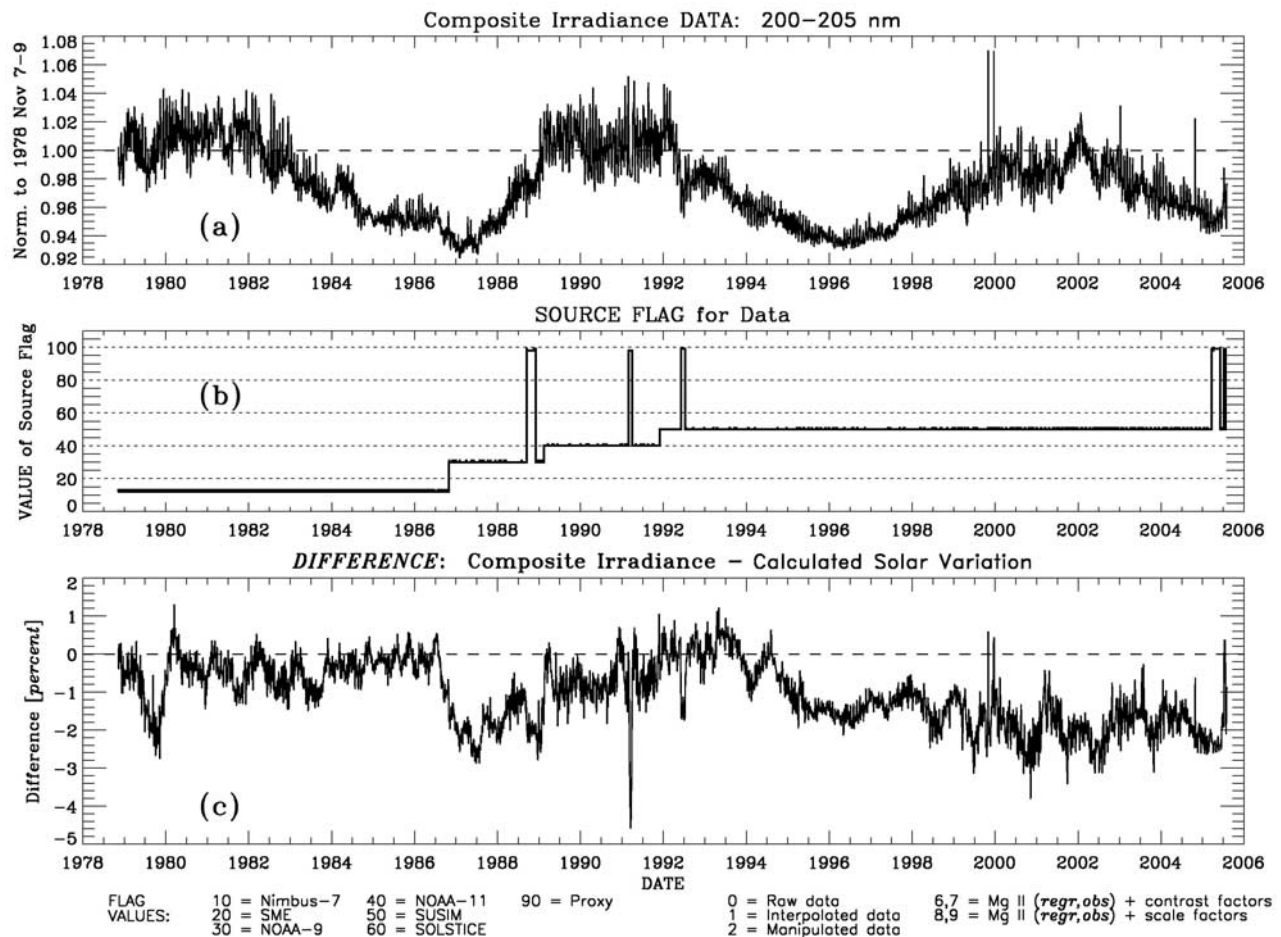


Figure 10. Composite spectral irradiance time series at 200–205 nm. (a) Irradiance data normalized to November 1978. (b) Data source flag for each daily sample. (c) Relative irradiance difference between the composite irradiance data and calculated proxy values using the 2-component model (in percent), smoothed with a 5-day running average.

data gap is to be filled, the reference irradiance value of the replacement data is determined by averaging the instrument irradiance data samples for the three days prior to the gap, then extracting only those values needed to fill the gap. For the 120–170 nm spectral interval from November 1978 to December 1981, where no prior data are available, the normalization is based on the first three days of SME data in July 1982, because the initial SME data in early 1982 show excessive drift relative to solar proxy estimates. The accuracy of this procedure depends on the magnitude of day-to-day noise in the instrument irradiances and any short-term variations in solar activity prior to the data gap. No normalization is calculated between the synthetic values at the end of a data gap and the observed data following the gap.

4.4. Determination of Absolute and Time-Dependent Uncertainties

[38] Assigning uncertainty values to the data in the composite spectral irradiance data set is particularly challenging because of the variety of instruments used, the normalization procedure employed in section 2.2, and the merging of data sets in wavelength and time. For absolute

uncertainty values, we use the root-sum-square (RSS) combination of the individual instrument uncertainty values and the uncertainty of the normalization spectrum by *Thuillier et al.* [2004]. In periods where synthetic data are used for the composite irradiance product, the absolute uncertainty is represented by the values in the study of *Thuillier et al.* [2004]. For time-dependent uncertainty values, we use the estimated values for each instrument in the appropriate spectral range. Synthetic data time-dependent uncertainty values are based on the Mg II index estimated uncertainty discussed by *Viereck et al.* [2004], contrast ratio standard deviations of 3–5% (T. Woods, private communication, 2008), and scale factor standard deviations reported in the study of *DeLand and Cebula* [1993]. We have not tried to reconcile these various data sets with each other, so users should understand that the final uncertainty data set will show spectral and temporal steps.

5. Evaluation and Validation

5.1. Time Series Comparisons (Internal)

[39] Figures 9–10 show examples of the composite irradiance data set created by the process described in section 4. Figure 9a shows the irradiance time series

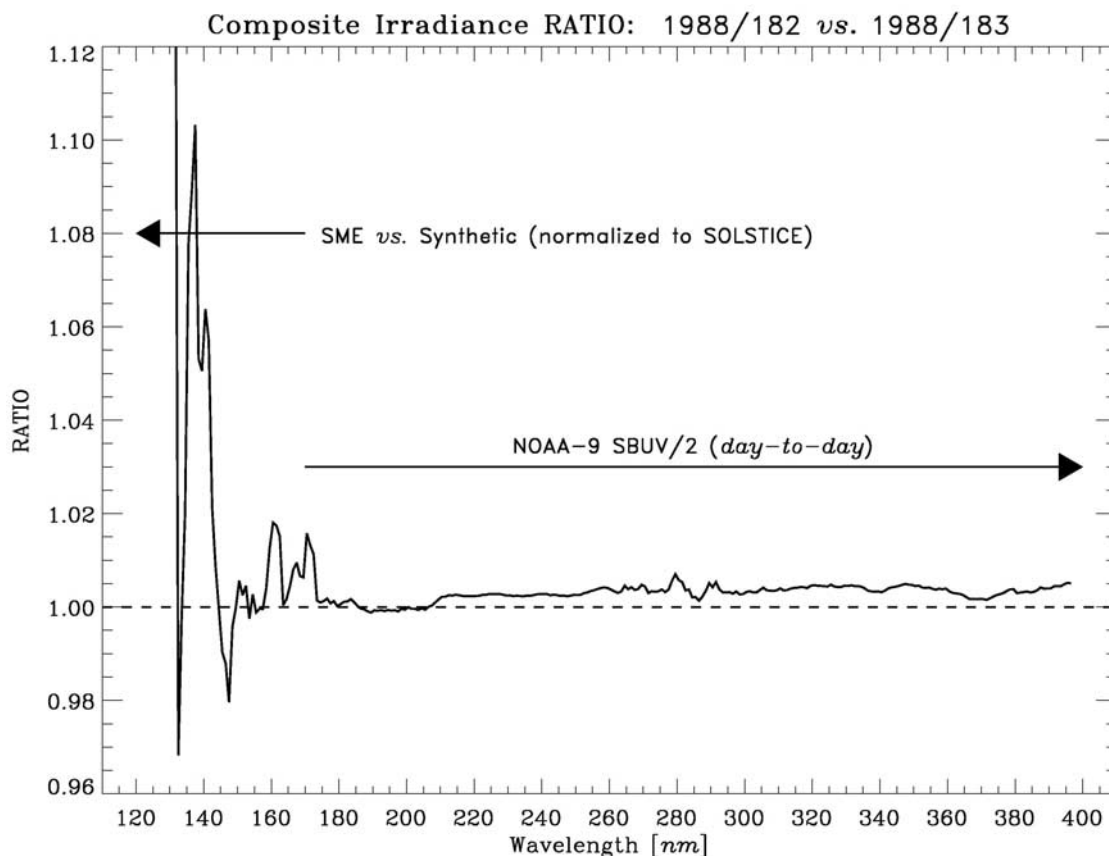


Figure 11. Ratio of spectra from the composite spectral irradiance data set for 1988 day 182 and 1988 day 183. The 120–170 nm region represents the transition from SME data to synthetic data. The 170–400 nm region represents a comparison of consecutive NOAA-9 SBUV/2 daily spectra. A 7-nm running average of the irradiance ratio is shown.

averaged over 150–154 nm, normalized to the average of the initial data points on 7–9 November 1978. Two multi year intervals and three smaller data gaps are filled with synthetic data. Figure 9b shows the time history of the source flag for these data. Flag values of 96 and 97 indicate data gaps filled using proxy calculations, values of 20 indicate SME data, values of 60 and 61 indicate UARS SOLSTICE data (observed and interpolated across small gaps, respectively), and values of 50 and 51 indicate UARS SUSIM data. Figure 9c shows the difference between the composite irradiance time series and the calculated proxy irradiance values for this wavelength band. There is some apparent small-scale structure in the long proxy replacement periods (November 1978 to December 1981, July 1988 to November 1991) because the composite irradiance values were calculated for each 1 nm bin and then averaged, whereas the proxy irradiance values for this comparison were calculated by first averaging the relevant contrast factors, then creating synthetic irradiance values. The absolute level of the solar minima for Cycle 21 in 1985–1986 and Cycle 22 in 1996 agree to within 2–3%, which is well within the long-term uncertainty of these data. This result is consistent with other solar activity indicators, such as He II 1083 nm equivalent width and magnetic flux, that show no significant change in solar minimum values between cycles 21 and 22. Some sharp features and steps in the difference

time series correspond to transitions between different data sets (e.g., January 1982, July 1988), although this does not hold true for every transition. The magnitude of such steps gives an indication of the accuracy of the original long-term characterization corrections for each instrument and the effectiveness of the normalization process. We note that the SME data also show uncorrected drifts and step changes of 3–6% during 1985–1988.

[40] A second example of the merged composite spectral irradiance time series is shown in Figure 10 for 200–205 nm. This time series incorporates data from four separate instruments (Nimbus-7 SBUV, NOAA-9 SBUV/2, NOAA-11 SBUV/2, UARS SUSIM), and fills three significant gaps with synthetic data. The amplitude of the maximum irradiance values for solar cycle 23 appears to be ~ 1 –2% less than the amplitude of cycles 21 and 22 (Figure 10a). This is again consistent with results from other solar activity indicators, such as sunspot number and magnetic flux. In this example, the transitions between different instruments show steps of 1% or less in the difference time series (Figure 10c), while the synthetic data intervals are 1–2% low. We have applied a correction for the quasi-annual periodic oscillation in the Nimbus-7 SBUV data as discussed in the study of *DeLand and Cebula* [2001], but there appears to be a residual feature at the 1% level during 1980–1986.

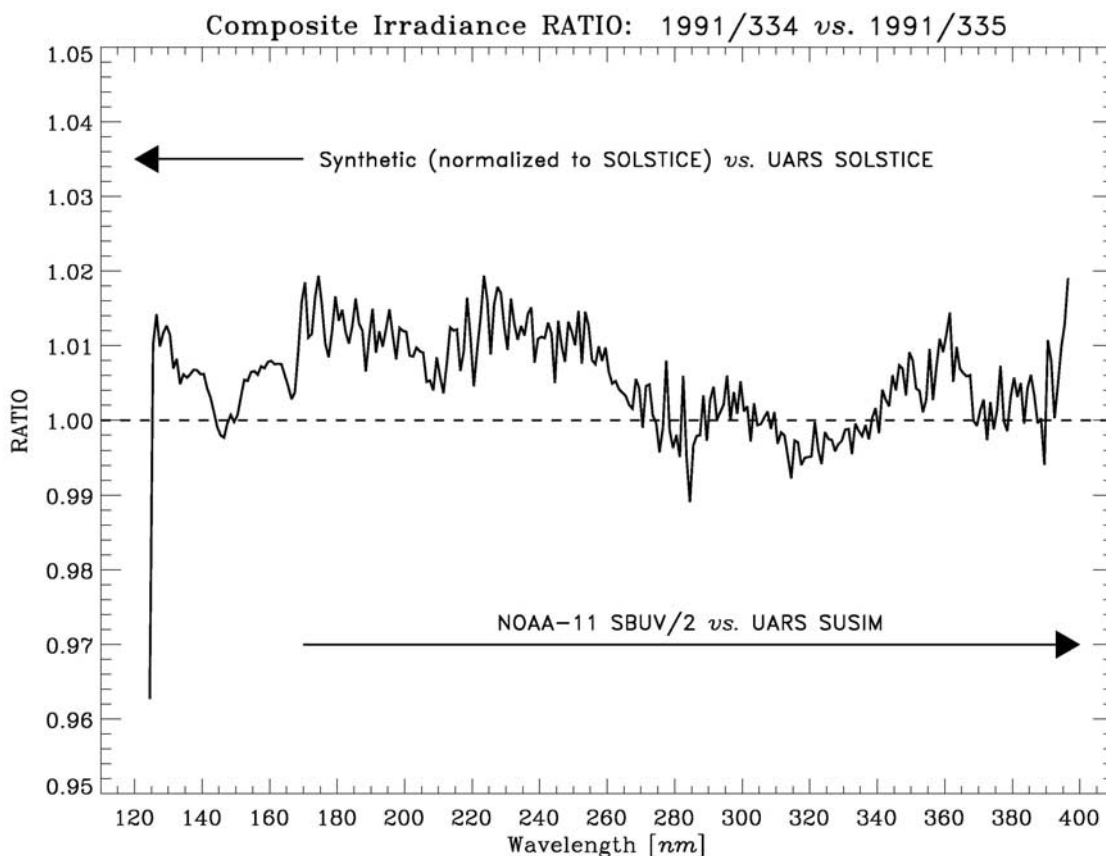


Figure 12. Ratio of spectra from the composite spectral irradiance data set for 1991 day 334 and 1991 day 335. The 120–170 nm region represents the transition from synthetic data to SOLSTICE data. The 170–400 nm region represents the transition from NOAA-11 data to SUSIM data. A 7-nm running average of the irradiance ratio is shown.

[41] We have not attempted to produce a formal spectral and temporal uncertainty estimate for the composite spectral irradiance data set, as discussed in section 4.4. One estimate of spectral uncertainty comes from the remaining biases in inter-instrument comparison plots such as Figure 6c. Most comparisons show agreement to $\pm 1\%$ for 5 nm wavelength averages, with some biases reaching $\pm 2\%$ and only a few cases exceeding this range. As noted in section 3.2, we generally considered a difference time series drift of approximately 2% as a threshold for rejecting a data set. Section 5.3 presents further discussion of time-dependent uncertainties in the final composite spectral irradiance product.

5.2. Spectral Comparisons (Internal)

[42] Another method of evaluating the quality of the composite spectral irradiance data set is to take the ratio of spectra across a transition between instruments, using two dates close together to minimize any solar activity variations. An example of such a comparison is shown in Figure 11 for 1988 days 182 and 183. The 120–170 nm wavelength range represents the transition between SME data and synthetic data normalized to the end of the SME data set. There is some structure with amplitudes of ± 2 –4% between 140–170 nm, but no substantial offset. Since the normalization process for the synthetic data uses the average

of three consecutive days (1988 days 180–182) prior to the gap being filled, this structure provides an indication of the day-to-day variations in the SME data at the end of its record. For the 170–400 nm wavelength range, both dates use NOAA-9 SBUV/2 data. Solar activity variations between consecutive days may reach $\sim 1\%$ at 170–207 nm, decrease to $\sim 0.5\%$ at 208–260 nm, and are normally 0.1% or less at 290–400 nm. Differences at the 0.5% level for near-UV wavelengths are thus likely to be dominated by instrument precision.

[43] A second example of the spectral ratio comparison at a transition point is shown in Figure 12 for 1991 days 334 and 335. The 120–170 nm wavelength range compares synthetic data with UARS SOLSTICE data, where the synthetic data were referenced to SME in June 1988. The 170–400 nm wavelength range represents the ratio between NOAA-11 SBUV/2 and UARS SUSIM data. The smoothed spectral ratio shows agreement to less than 2%, suggesting that the normalization of each data set in March 1992 adopted in section 2.2 is accurate to $\sim 1\%$.

5.3. External Validation

[44] A typical method of validating a long-term satellite data set is to compare its behavior with a concurrent well-calibrated data set. This is not practical for the composite spectral irradiance product because essentially all appropri-

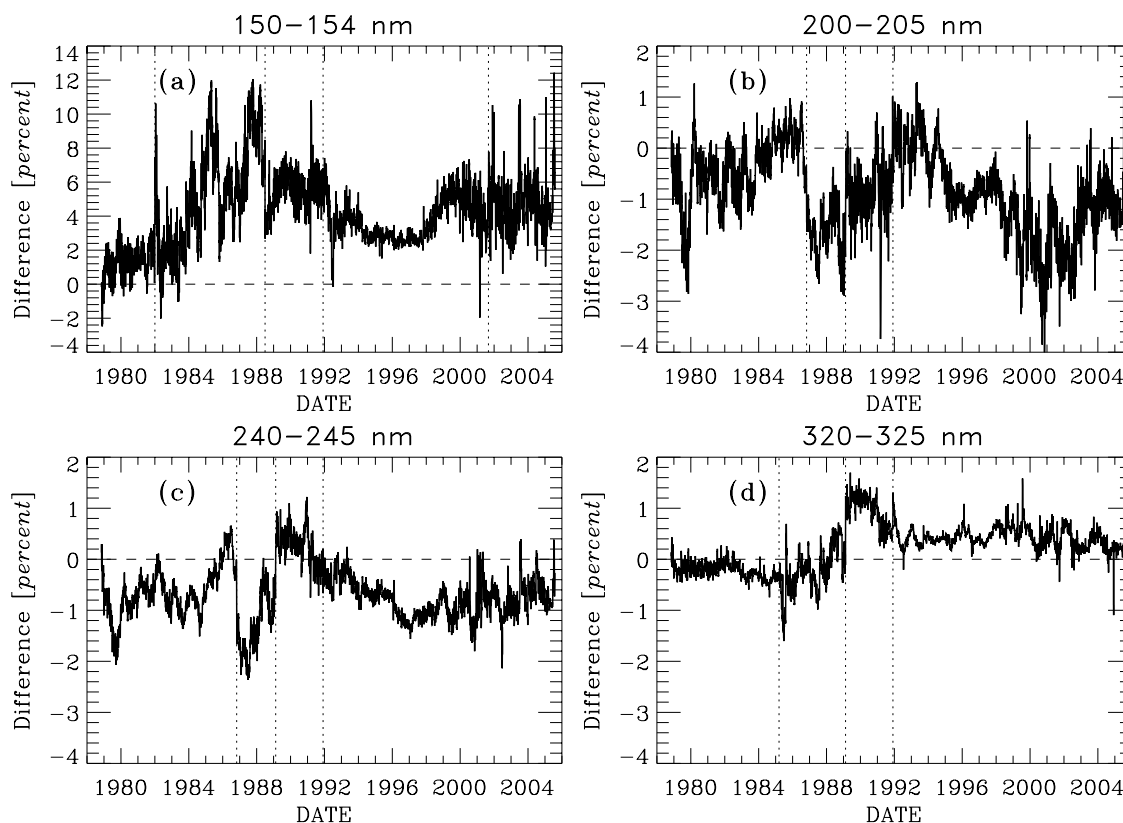


Figure 13. Irradiance time series differences (in percent) between the composite spectral irradiance data set and the synthetic irradiance data set by *Lean et al.* [2005] for different wavelength bands. (a) 150–154 nm. (b) 200–205 nm. (c) 240–245 nm. (d) 320–325 nm. All time series are smoothed with a 5-day running average. The dotted vertical lines indicate the locations of major instrument transitions for each wavelength band, as shown in Figure 8.

ate UV irradiance data sets are either already in use, or have been rejected for reasons discussed in Tables A1–A3. However, synthetic irradiance data sets can be created using proxy indexes to represent solar activity. One example of this process is the irradiance data set first created by *Lean et al.* [1997], and later revised by *Lean et al.* [2005]. For these data products, parametric relationships have been derived between detrended time series of irradiance data and proxy activity indicators for different spectral regions (Mg II index to represent bright plages and faculae, 10.7 cm flux to represent X-ray coronal emissions, sunspot blocking function to represent near-UV sunspot effects). The calculated synthetic irradiance data values implicitly assume that the quantitative relationships derived from rotational variations are applicable to solar cycle timescales. This assumption is consistent with the method used for the 2-component model by *DeLand and Cebula* [1993], while the 3-component model by *Woods et al.* [2000] also includes a term for facular network growth and decay timescales. We note that neither of these studies used explicitly detrended irradiance data, as was done in the study of *Lean et al.* [1997].

[45] We have created systematic time series comparisons between our composite irradiance product and the *Lean et al.* synthetic irradiance data set, analogous to the comparisons discussed in sections 3.1 and 3.2. Examples of the time series differences for selected wavelength bands are shown in Figure 13. For most wavelength bands and time

periods, the differences lie between $\pm 2\%$, which falls within the typical long-term uncertainty for the composite irradiance data (note the larger scale for the 150–154 nm comparison in Figure 13a). Some larger differences observed at 120–170 nm in 1985 and 1988 probably indicate remaining issues with the SME irradiance data.

[46] The time-dependent structure in Figure 13a between 1992–2000 has a phase that matches the solar activity cycle. This structure is present with an amplitude of 2–4% for wavelength bands between 125–170 nm. Our composite spectral irradiance product uses SOLSTICE V18 data in this region, whereas the synthetic irradiance data set is based on an analysis of SOLSTICE V8 data collected between December 1991 and September 1994 [*Lean et al.*, 1997]. The scaling coefficients based only on data from the descending portion of Cycle 22 may not fully represent the FUV solar cycle irradiance variation. A full analysis of irradiance scaling coefficients appropriate for our data set is beyond the scope of this paper, but certainly offers some interesting possibilities.

[47] The overall agreement between the composite spectral irradiance data set and the *Lean et al.* synthetic data set can be visualized by examining a two-dimensional difference time series plot (Figure 14), where wavelength is shown on the Y-axis. The data have been binned in 5 nm wavelength bands, with slight adjustments near sharp features in the irradiance spectrum, and 10-day time incre-

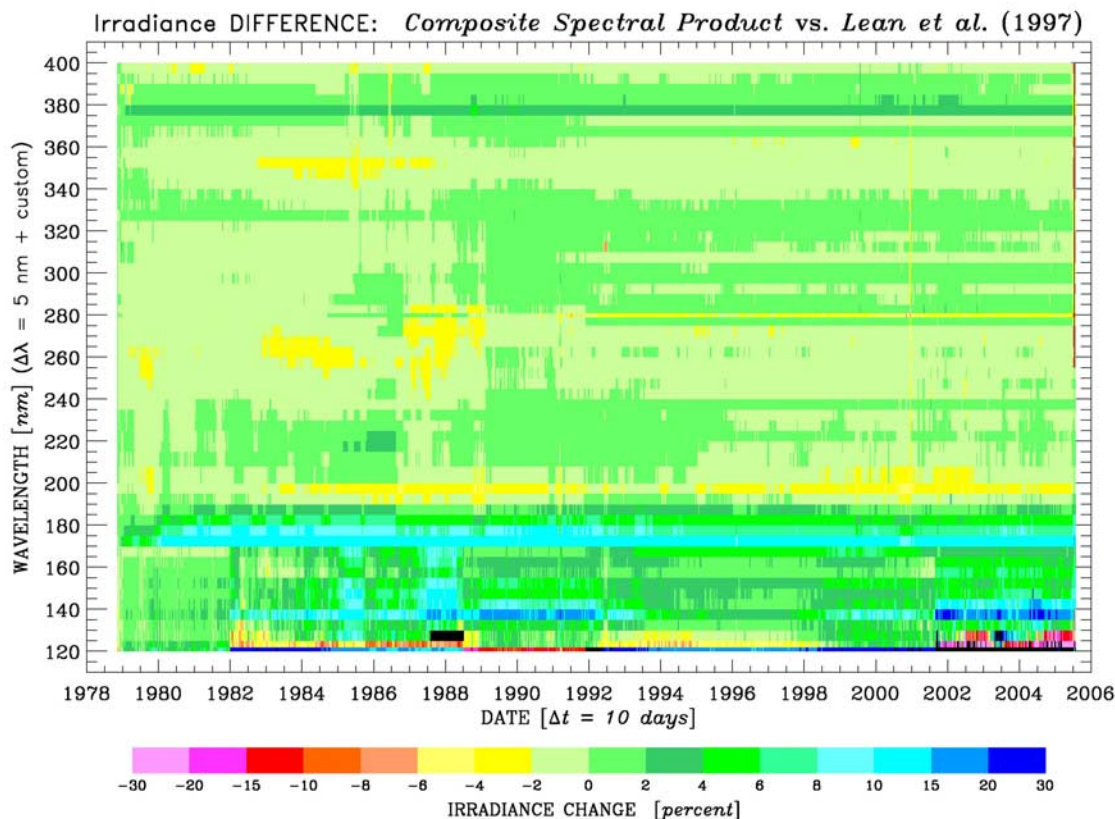


Figure 14. Irradiance time series differences (in percent) between the composite spectral irradiance data set and the synthetic irradiance data set by *Lean et al.* [2005] for the wavelength range 120–400 nm using 5 nm bands. The temporal binning is 10 days.

ments. For $\lambda > 190$ nm, most of the differences fall within the $\pm 2\%$ range, as noted previously. These differences may represent limitations with either the composite irradiance data set or the *Lean et al.* model. Larger difference values at 170–190 nm reflect uncorrected errors in the Nimbus-7 SBUV calibration, as discussed in the study of *DeLand and Cebula* [2001].

6. Remaining Issues and Conclusion

[48] The composite spectral irradiance data set presented in this paper was constructed from six independently measured data sets collected over more than 25 years. While it represents the best data products that are available, we acknowledge that there are some features in the individual instrument data sets that clearly fall outside the range of likely solar behavior. Examples include the step changes

in SME data during 1985–1988, the large initial positive drift in Nimbus-7 SBUV data at 170–190 nm during 1979–1980, and the jump at the transition between SOLSTICE and SUSIM data at 120–150 nm in 2001. If the decision is made to “intervene” and improve the quality of these data, some difficult questions arise. What are the criteria by which the original data are judged to have been corrected? What is the threshold beyond which such intervention can be justified? We have chosen to produce and distribute a composite spectral irradiance data set containing no alterations to the original data beyond absolute adjustments and published recommendations. Further changes to this data set will be discussed with the respective instrument teams, and any revisions will be announced to the user community.

[49] The current composite UV irradiance data product created from this project is available online at the LASP Interactive Solar Irradiance Datacenter (LISIRD, <http://>

Table A1. Data Set Matrix for 120–170 nm^a

Time Range	Data Sets Available	Comments
November 1978 to December 1981 January 1982 to June 1988	Synthetic SME	Data values created using Mg II index + 3-component model. 5% drop in first half of 1982 at 150–170 nm. Short-term increase of 5–6% in 1985 at 130 nm, 140–170 nm. 5–10% jump after mid-1987 at 125–155 nm.
July 1988 to November 1991	Synthetic	Data values created using Mg II index + 3-component model. Scaled He II 1083 nm values used to fill Mg II data gaps in September to November 1988, March 1991.
December 1991 to August 2001	SOLSTICE , SUSIM	SOLSTICE data have less noise for $\lambda < 150$ nm, although some narrow wavelength bands ($\Delta\lambda = 2$ nm) show fluctuations of 5%.
August 2001 to July 2005	SUSIM	Data quality decreases at $\lambda < 140$ nm because of known scattered light problems.

^aBoldface entry in column 2 indicates data set used in composite irradiance product.

Table A2. Data Set Matrix for 170–300 nm^a

Time Range	Data Sets Available	Comments
November 1978 to December 1981	Nimbus-7	Quasi-annual periodic oscillation at 170–260 nm corrected using empirical function. Residual error has 1% or less peak-to-peak amplitude. Rapid initial drift observed in 1979–1980 at 170–190 nm (+10% at 170 nm, decreasing to zero at 190 nm).
January 1982 to March 1985	Nimbus-7 , SME	SME values drift higher by ~5% at $\lambda < 210$ nm (also seen in proxy comparisons for $\lambda < 190$ nm). SME data have larger day-to-day noise. SME data also show decreases of 5% at 220–225 nm, 235–240 nm.
March 1985 to October 1986	Nimbus-7 , SME, NOAA-9	SME data show short-term increase of 5–6% in mid-1985 at $\lambda < 200$ nm. NOAA-9 has dip and noise in mid-1985. NOAA-9 data have a decrease of 2–4% and increased noise in mid-1985 because of goniometry errors. Similar problem seen in mid-1986 at $\lambda < 260$ nm.
October 1986 to June 1988	SME, NOAA-9	SME data show drifts of 2–4%. NOAA-9 comparisons with 2-component model agree to within $\pm 2\%$. SME differences are larger and show more noise.
July 1988 to February 1989	NOAA-9	Data gap in September to November 1988 filled by synthetic data. No obvious anomalies.
February 1989 to November 1991	NOAA-9, NOAA-11	Relative drifts between instruments $< \pm 2\%$. NOAA-9 has data gaps due to near-terminator orbit in 1990–1991. NOAA-11 data drift by ~2% vs. 2-component model during 1989 at 170–180 nm, 190–215 nm. Both instruments have data gap in March 1991.
December 1991 to October 1994	NOAA-9, NOAA-11, SOLSTICE, SUSIM	NOAA-9 data show problems due to near-terminator orbit through early 1992, additional data gap in August 1993. NOAA-11 drifts of 1–2% continue, data gaps due to drift into near-terminator orbit appear in 1993–1994. SUSIM data agree with 2-component model predictions to $< \pm 2\%$. SOLSTICE drifts vs. 2-component model at 235–270 nm begin to appear in 1994. UARS data gap affects SUSIM and SOLSTICE in June to July 1992.
October 1994 to May 1997	NOAA-9, SOLSTICE, SUSIM	NOAA-9 has additional data gaps in 1995 and 1996, increased noise after mid-1996. SUSIM has decreases up to –2% at 170–215 nm. SOLSTICE drift vs. 2-component model at 235–270 nm grows to –3% by 1997.
May 1997 to August 2001	SOLSTICE, SUSIM	SUSIM drift vs. 2-component model at 175–215 nm grows slightly, reaches –3% in places. SOLSTICE drift vs. 2-component model at 235–270 nm grows to –6% at 255–260 nm, less at shorter and longer wavelengths. SOLSTICE noise increases beginning in 1999, with more noise and gaps after late 2000 (star tracker failed in September 2000).
August 2001 to July 2005	SUSIM	Performance remains consistent, with more data gaps due to UARS power issues in 2005.

^aBoldface entry in column 2 indicates data set used in composite irradiance product.

lasp.colorado.edu/lisird/). We have provided a basic summary of the data set at this location, along with simple IDL software to read the data and extract individual spectra or irradiance time series. High quality UV irradiance measurements from the SIM and SOLSTICE II instruments on the SORCE satellite begin in February 2003 and continue to the present, providing more than two years of overlap with the final portion of our composite UV irradiance data set. We

anticipate using these data in the future to produce an extended version of our data set.

Appendix A

[50] Tables A1, A2, and A3 contain brief summaries of the instrument intercomparison and proxy model comparison results that were used to select the data sets for each

Table A3. Data Set Matrix for 300–400 nm^a

Time Range	Data Sets Available	Comments
November 1978 to March 1985	Nimbus-7	Some drift vs. 2-component model observed in narrow bands (e.g., –3% at 353 nm, +3% at 376 nm). –1% changes observed at 340 nm and 360 nm.
March 1985 to October 1986	Nimbus-7, NOAA-9	Nimbus-7 drift continues at 340–360 nm, expands in 380–400 nm region. NOAA-9 data have no major drift, frequent $\pm 1\%$ fluctuations are due to goniometry errors.
October 1986 to February 1989	NOAA-9	NOAA-9 data have no major drift, frequent $\pm 1\%$ fluctuations are due to goniometry errors.
February 1989 to November 1991	NOAA-9, NOAA-11	NOAA-11 data have slightly better noise behavior. Use of NOAA-11 data provides continuity with 170–300 nm data choice.
December 1991 to October 1994	NOAA-9, NOAA-11, SUSIM	NOAA-11 long-term drifts are $< 1\%$. SUSIM long-term drifts are $\pm 1\%$. Use of SUSIM data provides continuity with 170–300 nm data choice.
October 1994 to May 1997	NOAA-9, SUSIM	NOAA-9 short-term noise increases to $\pm 2\%$ in 1996–1997. SUSIM has more drift at 392–394 nm than at other wavelengths. Use of SUSIM data provides continuity with 170–300 nm data choice.
May 1997 to July 2005	SUSIM	No significant drift issues.

^aBoldface entry in column 2 indicates data set used in composite irradiance product. Note that SOLSTICE data are not listed here because the instrument characterization at 300–400 nm was explicitly forced to have no long-term changes.

temporal and spectral interval in the composite spectral irradiance data set.

[51] **Acknowledgments.** This work has benefited greatly from informative discussions with the respective instrument scientists: Don Heath and Barry Schlesinger for Nimbus-7 SBUV, Gary Rottman for SME, Tom Woods for UARS SOLSTICE, and Linton Floyd for UARS SUSIM. Gerard Thuillier provided valuable assistance with the use of the reference solar irradiance spectrum. The focus and readability of this article were improved by comments from two anonymous reviewers. The raw SBUV/2 data were obtained from NOAA/NESDIS with support from the NOAA Climate and Global Change Atmospheric Chemistry Element. This work was supported by the NASA Living With a Star Targeted Research and Technology program through grant NNH05CC17C.

[52] Amitava Bhattacharjee thanks Claus Frohlich and another reviewer for their assistance in evaluating this paper.

References

- Bengtsson, L. (2006), On the response of the climate system to solar forcing, *Space Sci. Rev.*, *125*, 187–197.
- Cebula, R. P., M. T. DeLand, E. Hilsenrath, B. M. Schlesinger, R. D. Hudson, and D. F. Heath (1991), Intercomparisons of the solar irradiance measurements from the Nimbus-7 SBUV, the NOAA-9 and NOAA-11 SBUV/2, and the STS-34 SSBUV instruments: A preliminary assessment, *J. Atmos. Terr. Phys.*, *53*, 993–997.
- Cebula, R. P., G. O. Thuillier, M. E. VanHoosier, E. Hilsenrath, M. Herse, G. E. Brueckner, and P. C. Simon (1996), Observations of the solar irradiance in the 200–350 nm interval during the ATLAS-1 mission: A comparison among three sets of measurements—SSBUV, SOLSPEC, and SUSIM, *Geophys. Res. Lett.*, *23*, 2289–2292.
- Cebula, R. P., M. T. DeLand, and E. Hilsenrath (1998), NOAA 11 Solar Backscattered Ultraviolet, model 2 (SBUV/2) instrument solar spectral irradiance measurements in 1989–1994. 1: Observations and long-term calibration, *J. Geophys. Res.*, *103*, 16,235–16,249.
- Crooks, S. A., and L. J. Gray (2005), Characterization of the 11-year solar signal using a multiple regression analysis of the ERA-40 dataset, *J. Clim.*, *18*, 996–1015.
- DeLand, M. T., and R. P. Cebula (1993), Composite Mg II solar activity index for solar cycles 21 and 22, *J. Geophys. Res.*, *98*, 12,809–12,823.
- DeLand, M. T., and R. P. Cebula (1998), NOAA 11 Solar Backscattered Ultraviolet, model 2 (SBUV/2) instrument solar spectral irradiance measurements in 1989–1994. 2: Results, validation, and comparisons, *J. Geophys. Res.*, *103*, 16,251–16,273.
- DeLand, M. T., and R. P. Cebula (2001), Spectral solar UV irradiance data for cycle 21, *J. Geophys. Res.*, *106*, 21,569–21,583.
- DeLand, M. T., R. P. Cebula, and E. Hilsenrath (2004a), Observations of solar spectral irradiance change during cycle 22 from NOAA-9 Solar Backscattered Ultraviolet Model 2 (SBUV/2), *J. Geophys. Res.*, *109*, D06304, doi:10.1029/2003JD004074.
- DeLand, M. T., L. E. Floyd, G. J. Rottman, and J. M. Pap (2004b), Status of UARS solar UV irradiance data, *Adv. Space Res.*, *34*, 243–250.
- Dewitte, S., D. Crommelnyck, S. Mekaoui, and A. Joukoff (2004), Measurement and uncertainty of the long-term total solar irradiance trend, *Solar Phys.*, *224*, 209–216.
- Floyd, L. E., D. K. Prinz, P. C. Crane, and L. C. Herring (2002), Solar UV irradiance variation during cycles 22 and 23, *Adv. Space Res.*, *29*, 1957–1962.
- Frohlich, C. (2006), Solar irradiance variability since 1978, *Space Sci. Rev.*, *125*, 53–65.
- Harvey, J. W. (1984), Helium 10830 Å irradiance: 1975–1983, in *Solar Irradiance Variations on Active Region Time Scales*, edited by B. J. Labonte et al., *NASA Conf. Publ.*, 2310, 197–211.
- Lean, J. L., G. J. Rottman, H. L. Kyle, T. N. Woods, J. R. Hickey, and L. C. Puga (1997), Detection and parameterization of variations in solar mid and near ultraviolet radiation (200 to 400 nm), *J. Geophys. Res.*, *102*, 29,939–29,956.
- Lean, J., G. Rottman, J. Harder, and G. Kopp (2005), SORCE contributions to new understanding of global change and solar variability, *Solar Phys.*, *230*, 27–53.
- Meier, R. R. (1991), Ultraviolet spectroscopy and remote sensing of the upper atmosphere, *Space Sci. Rev.*, *58*, 1–185.
- Rottman, G. J. (1988), Observations of solar UV and EUV variability, *Adv. Space Res.*, *8*(7), 53–66.
- Rottman, G. J. (2005), The SORCE mission, *Solar Phys.*, *230*, 7–25.
- Rottman, G., T. Woods, M. Snow, and G. DeToma (2001), The solar cycle variation in ultraviolet irradiance, *Adv. Space Res.*, *27*, 1927–1932.
- Schlesinger, B. M., and R. P. Cebula (1992), Solar variation 1979–1987 estimated from an empirical model for changes with time in the sensitivity of the solar backscatter ultraviolet instrument, *J. Geophys. Res.*, *97*, 10,119–10,134.
- Skupin, J., S. Noël, M. W. Wuttke, M. Gottwald, H. Bovensmann, M. Weber, and J. P. Burrows (2005), SCIAMACHY solar irradiance observation in the spectral range from 240 to 2380 nm, *Adv. Space Res.*, *35*, 370–375.
- Tapping, K. F. (1987), Recent solar radio astronomy at centimeter wavelengths: The temporal variability of the 10.7 cm flux, *J. Geophys. Res.*, *92*, 829–838.
- Thuillier, G., L. Floyd, T. N. Woods, R. Cebula, E. Hilsenrath, M. Herse, and D. Labs (2004), Solar irradiance reference spectra, in *Solar Variability and its Effects on Climate*, *Geophys. Monogr.*, vol. 141, AGU, Washington, D. C., pp. 171–194.
- Viereck, R., and L. C. Puga (1999), The NOAA Mg II core-to-wing solar index: Construction of a 20-year time series of chromospheric variability from multiple satellites, *J. Geophys. Res.*, *104*, 9995–10,005.
- Viereck, R. A., L. E. Floyd, P. C. Crane, T. N. Woods, B. G. Knapp, G. Rottman, M. Weber, L. C. Puga, and M. T. DeLand (2004), A composite Mg II index spanning from 1978 to 2003, *Space Weather*, *2*, S10005, doi:10.1029/2004SW000084.
- Weber, M., J. P. Burrows, and R. P. Cebula (1998), GOME solar UV/VIS irradiance measurements in 1995 and 1996—first results on proxy solar activity studies, *Solar Phys.*, *177*, 63–77.
- Willson, R. C., and A. V. Mordvinov (2003), Secular total solar irradiance trend during solar cycles 21–23, *Geophys. Res. Lett.*, *30*(5), 1199, doi:10.1029/2002GL016038.
- Woods, T. N., et al. (1996), Validation of the UARS solar ultraviolet irradiances: Comparisons with the ATLAS 1 and 2 measurements, *J. Geophys. Res.*, *101*, 9541–9569.
- Woods, T. N., W. K. Tobiska, G. J. Rottman, and J. R. Worden (2000), Improved solar Lyman α irradiance modeling from 1947 through 1999 based on UARS observations, *J. Geophys. Res.*, *105*, 27,195–27,215.
- Woods, T. N., et al. (2005), Solar EUV experiment (SEE): Mission overview and first results, *J. Geophys. Res.*, *110*, A01312, doi:10.1029/2004JA010765.

R. P. Cebula and M. T. DeLand, Science Systems and Applications, Inc., 10210 Greenbelt Road, Suite 600, Lanham, MD 20706, USA. (matthew_deland@ssaiahq.com)